Sensors and Actuators A 205 (2014) 53–57

Contents lists available at ScienceDirect

Sensors and Actuators A: Physical

journal homepage: www.elsevier.com/locate/sna

Computational study of slot photonic crystal ring-resonator for refractive index sensing

Fu-Li Hsiao*, Yu-Ting Ren

Institute of Photonics, National Changhua University of Education, Changhua, Taiwan

ARTICLE INFO

Article history:
Received 17 July 2013
Received in revised form 23 October 2013
Accepted 23 October 2013
Available online 31 October 2013

Keywords:
Photonic crystals
Slow light
Ring resonator
Refractive index sensor

ABSTRACT

We perform simulations of slot photonic crystal ring-resonators in dielectric media. The structure comprises two concentric photonic crystal ring waveguides. A slot of width of a few tens of nm is inserted between the inner and outer ring waveguides. By individually modifying the geometric parameters of inner and outer waveguides, the ring-resonator structure generates slow-light whispering-gallery resonance with an optical field concentrating within the slot area. As a sensing element, the structure exhibits advantages of both slow-light and ring-resonator devices. The estimated sensitivity is about 250 nm/refractive index unit and the minimum detectable refractive index variation is about 0.008.

1. Introduction

In recent years, sensing devices based on photonic crystal structures have received much attention. The spatially periodic modulated refractive index of a photonic crystal leads to unique dispersion relations characterized by photonic band gaps or slow-light propagation. Variations in the ambient refractive index result in changes to the dispersion relation and the optical properties of the photonic crystal. Refractive-index sensing can be achieved by measuring variations in the optical properties; for instance, the reflection or transmission spectra, of the device [1–3].

Photonic crystal slab-based sensing devices have been extensively studied. The structure of the photonic crystal slab consists of periodic holes arrayed in a dielectric slab. The slab usually has higher refractive index than the holes. Photonic crystal waveguides and cavities can be formed by inserting certain defects in the periodic holes. With excellent optical confinement capabilities, waveguides and resonators based on photonic crystal slab are quite efficient. The footprint of these devices is small. For sensing purposes, the structures are placed in solution with analytes; thus the surface and holes of the structure are covered and filled by the solution. The variation in refractive index resulting from the change in analytes can be quantified by characterizing the transmission spectra [4,5]. The sensitivity of a photonic crystal slab device is limited because the electromagnetic energy is mainly confined within the dielectric material rather than the ambient medium. The interaction between the light wave and ambient medium can be enhanced by inserting extra holes into the cavities [6–11] or slots into the waveguides.

Slow-light effects offer an alternative approach to enhance light–matter interaction [12,13]. Due to the extreme slow group velocity, the interaction between light and ambient medium can be significantly enhanced [12]. Group velocities can be dramatically slowed down in photonic crystal slabs and one-dimensional grating waveguides [14–16]. This has also been observed in photonic-crystal slot slow-light waveguides [13]. These slot slow-light waveguides consist of two parallel photonic crystal waveguides. A slot of a few tens of nanometers in width is sandwiched between the waveguides. The structure generates several flat photonic bands near the edge of the reduced Brillouin zone. One of these bands produces strong confinement of light in the slot area. Because of the slow-light effect and high energy density within the slot area, such a band exhibits a significant high sensitivity to refractive changes within the slot. Confining light in a nanometer-wide low-refractive-index void gap between waveguides has been reported [17]. Such structures are usually referred to slot waveguides. Slot waveguides enable the structure to confine light in a low-index region. Compact chemical or biochemical sensors based on slot waveguide structure have been reported [18,19]. The concept has been widely adopted in dual nanobeam photonic crystal devices [11,20–23]. The abovementioned slot slow-light waveguide is one example of these devices. The band-edge modes of a dual-beam structure split from the band-edge modes of the single-beam structure; i.e., each band-edge mode of a single beam splits into two modes when two beams are placed near to each other.

* Corresponding author at: No. 1, Jin De Road, Changhua City, Taiwan. Tel.: +886 4 7232105x3393; fax: +886 4 7211153.
E-mail address: fulihsiao@cc.ncue.edu.tw (F.-L. Hsiao).

0924-4247/$ – see front matter
http://dx.doi.org/10.1016/j.sna.2013.10.022

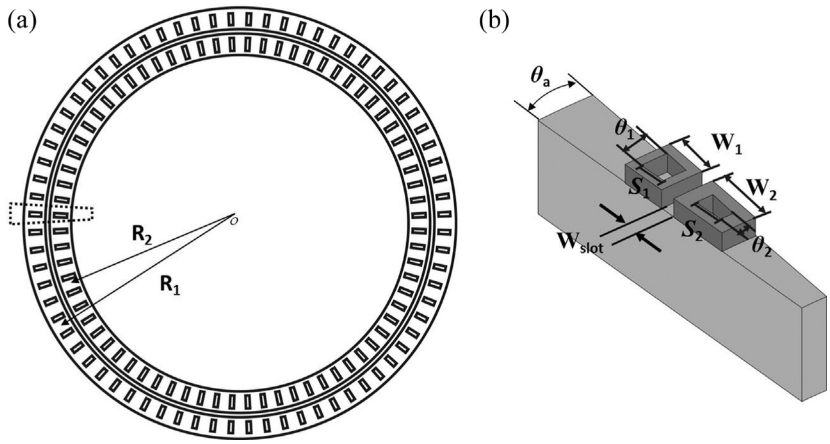

Fig. 1. (a) Sketch of the SPCR structure;(b) enlarged three-dimensional view of a unit cell.

The performance of an optical refractive-index-sensing device can be defined by two key parameters: sensitivity and minimum-detectable refractive-index variation. For most of the optical sensors based on the slow-light effect and resonance, the refractive index variation (Δn) is quantified by measuring the peak wavelength shift ($\Delta\lambda$). The sensitivity (S) of sensors can be express by: $S = \Delta\lambda/\Delta n$. Alternatively, the quality factor (Q) of slow light or the resonance peak is: $Q = \lambda/\Delta\lambda_{FWHM}$, where λ and $\Delta\lambda_{FEHM}$ are the center wavelength and full-width at half-maximum (FWHM) of the peak. We assume the minimum-detectable wavelength shift equals FWHM [9], and therefore the minimum-detectable refractive variation is $\Delta n_{min} = \lambda/(Q \times S)$. Optical sensor designers are pursuing high S and low Δn_{min}; S can be raised by enhancing light–matter interactions and Δn_{min} can be decreased by reducing FWHM or increasing sensitivity.

2. Design of slot photonic crystal ring-resonator

For this study, we performed simulations of a slot photonic crystal ring-resonator (SPCR). The major purpose of the SPCR structure is to generate the slow-light whispering-gallery modes. The resonant optical field is mainly confined within the slot region. Because the light is confined there rather than the dielectric material, one can expect that the SPCR has high sensitivity with respect to index changes in the slot. Nevertheless, the FWHM of resonance peaks of the SPCR will be reduced because of the whispering-gallery resonance. Therefore, Δn_{min} is expected to be reduced. The resonator, see Fig. 1(a), consists of two concentric photonic crystal ring waveguides, the radii of outer and inner are R_1 and R_2, respectively. A slot is sandwiched between these two waveguides. Periodic fan-shaped holes are patterned on both inner and outer ring waveguides. The structure is assumed to be fabricated on a silicon-on-insulator wafer. In the numerical simulations, the thicknesses of the device layer and buried oxide layer are assumed to be 230 nm and 2 μm, respectively. Fig. 1(b) is an enlarged three-dimensional view of a unit cell marked by the dash line in Fig. 1(a). The notation for the geometric parameters of the SPCR structure is as follows: the widths of the outer and inner ring waveguides are W_1 and W_2, respectively; the width of the slot between the waveguides is W_{slot}; the angular period of the fan-shaped holes on both ring waveguides is θ_a, i.e., the circular lattice constants of the outer and inner photonic crystal ring waveguides are $R_1 \times \theta_a$ and $R_2 \times \theta_a$, respectively. Each fan-shaped hole is an arc segment of a circular sector with vertex at the center of the two concentric ring waveguides. The fan-shaped holes are placed at the center of the waveguides. The fan angles of these holes for the outer and inner waveguides are θ_1 and θ_2, respectively. S_1 and S_2 denote the widths of these holes in the outer and inner waveguides, respectively.

The photonic crystal micro-ring resonator with single ring waveguide has been studied [24]. The dispersion for the photonic crystal ring waveguide can be expressed by the relation between the optical angular frequency and the wavevector projected onto the circumference. As mentioned above, the slow-light modes in the dual parallel and identical straight photonic crystal waveguides split from the modes in a single waveguide. However, the radii of inner and outer photonic crystal waveguides in the SPCR are not identical. To match the band-edge modes of the inner and outer photonic crystal ring waveguide, we have to modify the geometric parameters of each ring individually. The dispersion calculation is performed by the three-dimensional finite element method (FEM). We chose the eigen-frequencies analysis of commercial FEM software provided by COMSOL Multiphysics. Fig. 2(a) provides a sketch of the unit cell used in the dispersion calculations. The corresponding cylindrical coordinate system is also shown in Fig. 2(a). The silicon waveguide is laid over the SiO_2 substrate and opened to the air. Periodic boundary conditions with tunable phase difference, i.e., the wavevector, are adopted along the boundaries in the θ direction. The rest of the boundaries are set for low reflective conditions. We adopt triangular vector elements in FEM mesh generation. The maximum element sizes are as follows: 1/10 of W_{slot} in slot region, 1/10 of widths of ring waveguides, 1/10 of widths of holes in ring waveguides and 100 nm in the remaining calculation domain. In order to verify our simulation process, we calculated the dispersion of structure in Ref. [22]. Our simulated results agree very well with the dispersion in Ref. [22]. We define the circular lattice constant as $a = R \times \theta_a$, the length of fan-shaped holes as $L = R \times \theta_L$, where R is the radius of ring waveguide. In addition, the width of the waveguide and fan-shaped holes are W and S, respectively. The dependence on L for the lowest photonic band of single photonic crystal waveguide (Fig. 2(b)) shows band frequencies rising as L increases. Fig. 2(c) and (d) shows the variation of the lowest band with respect to S and W, respectively. In Fig. 2(c), increasing S results in a significant increase in frequency at the band edge, i.e., at reduced wave vector near 0.5. In contrast, from Fig. 2(d), increasing W results in frequency at the band edge decreasing. The variations of L, S, and W determine not only band frequency but also group velocities. According to the discussion above, the group velocities and frequencies of dispersion band can be controlled by modifying the geometric parameters. The dispersion band of the inner and outer ring waveguides can be matched to each other by choosing appropriate geometric parameters individually.